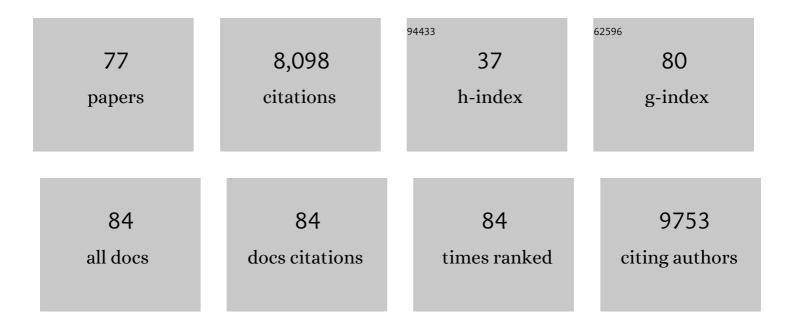
List of Publications by Year in descending order

Source: https://exaly.com/author-pdf/5366702/publications.pdf Version: 2024-02-01



FENG-CALLEL

#	Article	IF	CITATIONS
1	Construct high-precise SERS sensor by hierarchical superhydrophobic Si/Cu(OH)2 platform for ultratrace detection of food contaminants. Sensors and Actuators B: Chemical, 2022, 352, 131056.	7.8	8
2	Recent advances in the pre-oxidation process in electrocatalytic urea oxidation reactions. Chemical Communications, 2022, 58, 2430-2442.	4.1	71
3	Electrochemical reduction of nitrate on silver surface and an <i>in situ</i> Raman spectroscopy study. Inorganic Chemistry Frontiers, 2022, 9, 2734-2740.	6.0	18
4	Acceleration of the pre-oxidation process by tuning the degree of sulfurization for promoted oxygen evolution reaction. Chemical Communications, 2022, 58, 6360-6363.	4.1	23
5	Cerium-induced lattice disordering in Co-based nanocatalysts promoting the hydrazine electro-oxidation behavior. Chemical Communications, 2022, 58, 6845-6848.	4.1	15
6	Particle-in-Molybdenum Disulfide-Coated Cavity Structure with a Raman Internal Standard for Sensitive Raman Detection of Water Contaminants from Ions to <300 nm Nanoplastics. Journal of Physical Chemistry Letters, 2022, 13, 5815-5823.	4.6	22
7	Reduction-induced surface reconstruction to fabricate cobalt hydroxide/molybdenum oxide hybrid nanosheets for promoted oxygen evolution reaction. Chemical Engineering Journal, 2021, 413, 127540.	12.7	25
8	Integrated accurate extraction and fast detection of analyte: Capillarity-Based SERS substrate using in effluent monitoring. Applied Surface Science, 2021, 542, 148735.	6.1	5
9	Electronic Optimization by Coupling FeCo Nanoclusters and Pt Nanoparticles to Carbon Nanotubes for Efficient Hydrogen Evolution. ACS Sustainable Chemistry and Engineering, 2021, 9, 5895-5901.	6.7	9
10	Multiscale structure enabled effective plasmon coupling and molecular enriching for SERS detection. Applied Surface Science, 2021, 544, 148908.	6.1	11
11	SERS substrate with wettability difference for molecular self-concentrating detection. Nanotechnology, 2021, 32, 375603.	2.6	4
12	Heterostructured CuO@ZnO@Ag biomimetic setaria as wettability-switchable difunctional SERS substrate for trace pesticide and DNA detections. Nanophotonics, 2021, 10, 2671-2682.	6.0	11
13	Heterostructured Cu2O–Au nanowire as a dual-functional nanocomposite for environmental pollutant degradation and hydrogen peroxide sensing. Applied Optics, 2021, 60, 5936.	1.8	0
14	Preparation of a superhydrophobic AgNP/GF substrate and its SERS application in a complex detection environment. Optics Express, 2021, 29, 34085.	3.4	4
15	A self-sacrificial templated route to fabricate CuFe Prussian blue analogue/Cu(OH)2 nanoarray as an efficient pre-catalyst for ultrastable bifunctional electro-oxidation. Chemical Engineering Journal, 2021, 422, 130139.	12.7	58
16	Electrochemical synthesis of ammonia by nitrate reduction on indium incorporated in sulfur doped graphene. Chemical Engineering Journal, 2021, 426, 131317.	12.7	40
17	Dressing Plasmons in Nanoparticle-in-Quasi-Cavity Architectures for Trace-Level Surface-Enhanced Raman Spectroscopy Detection. ACS Applied Nano Materials, 2021, 4, 152-158.	5.0	2
18	"Pit-dot―ultrathin nanosheets of hydrated copper pyrophosphate as efficient pre-catalysts for robust water oxidation. Chemical Communications, 2021, 57, 11517-11520.	4.1	15

#	Article	IF	CITATIONS
19	Molten-Salt-Protected Pyrolytic Approach for Fabricating Borate-Modified Cobalt–Iron Spinel Oxide with Robust Oxygen-Evolving Performance. ACS Sustainable Chemistry and Engineering, 2021, 9, 14596-14604.	6.7	19
20	Cobalt, iron co-incorporated Ni(OH) <sub>2</sub> multiphase for superior multifunctional electrocatalytic oxidation. Chemical Communications, 2021, 57, 13752-13755.	4.1	4
21	Fast multiphase analysis: Self-separation of mixed solution by a wettability-controlled CuO@Ag SERS substrate and its applications in pollutant detection. Sensors and Actuators B: Chemical, 2020, 307, 127663.	7.8	22
22	Hierarchical Particle-In-Quasicavity Architecture for Ultratrace <i>In Situ</i> Raman Sensing and Its Application in Real-Time Monitoring of Toxic Pollutants. Analytical Chemistry, 2020, 92, 14754-14761.	6.5	118
23	Concurrently Realizing Geometric Confined Growth and Doping of Transition Metals within Graphene Hosts for Bifunctional Electrocatalysts toward a Solid-State Rechargeable Micro-Zn–Air Battery. ACS Applied Materials & Interfaces, 2020, 12, 38031-38044.	8.0	24
24	Molten-Salt-Protected Pyrolysis for Fabricating Perovskite Nanocrystals with Promoted Water Oxidation Behavior. ACS Sustainable Chemistry and Engineering, 2020, 8, 16711-16719.	6.7	17
25	Synthesis of Semiconducting 2H-Phase WTe <sub>2</sub> Nanosheets with Large Positive Magnetoresistance. Inorganic Chemistry, 2020, 59, 11935-11939.	4.0	17
26	Modulation of electronic structures in two-dimensional electrocatalysts for the hydrogen evolution reaction. Chemical Communications, 2020, 56, 11910-11930.	4.1	56
27	In-plane β-Co(OH) <sub>2</sub> /Co <sub>3</sub> O <sub>4</sub> hybrid nanosheets for flexible all-solid-state thin-film supercapacitors with high electrochemical performance. Nanoscale, 2020, 12, 24251-24258.	5.6	13
28	Novel (Ni, Fe)S2/(Ni, Fe)3S4 solid solution hybrid: an efficient electrocatalyst with robust oxygen-evolving performance. Science China Chemistry, 2020, 63, 1030-1039.	8.2	22
29	<p>In-situ Electrospinning for Intestinal Hemostasis</p> . International Journal of Nanomedicine, 2020, Volume 15, 3869-3875.	6.7	6
30	Modulation of crystal water in cobalt phosphate for promoted water oxidation. Chemical Communications, 2020, 56, 4575-4578.	4.1	37
31	Efficient Ammonia Electrosynthesis from Nitrate on Strained Ruthenium Nanoclusters. Journal of the American Chemical Society, 2020, 142, 7036-7046.	13.7	542
32	A molten-salt protected pyrolysis approach for fabricating a ternary nickel–cobalt–iron oxide nanomesh catalyst with promoted oxygen-evolving performance. Chemical Communications, 2020, 56, 4579-4582.	4.1	23
33	Nickel incorporated Co9S8 nanosheet arrays on carbon cloth boosting overall urea electrolysis. Electrochimica Acta, 2020, 338, 135883.	5.2	61
34	Electric Field-Modulated Surface Enhanced Raman Spectroscopy by PVDF/Ag Hybrid. Scientific Reports, 2020, 10, 5269.	3.3	11
35	An iron incorporation-induced nickel hydroxide multiphase with a 2D/3D hierarchical sheet-on-sheet structure for electrocatalytic water oxidation. Chemical Communications, 2019, 55, 10138-10141.	4.1	15
36	Modified bluing treatment to produce nickel–cobalt–iron spinel oxide with promoted oxygen-evolving performance. Chemical Communications, 2019, 55, 9841-9844.	4.1	18

#	Article	IF	CITATIONS
37	Promoted water splitting by efficient electron transfer between Au nanoparticles and hematite nanoplates: a theoretical and experimental study. Physical Chemistry Chemical Physics, 2019, 21, 1478-1483.	2.8	22
38	Constructing Hierarchical Wire-on-Sheet Nanoarrays in Phase-Regulated Cerium-Doped Nickel Hydroxide for Promoted Urea Electro-oxidation. , 2019, 1, 103-110.		100
39	Quasi Optical Cavity of Hierarchical ZnO Nanosheets@Ag Nanoravines with Synergy of Near- and Far-Field Effects for in Situ Raman Detection. Journal of Physical Chemistry Letters, 2019, 10, 3676-3680.	4.6	60
40	Copper-incorporated hierarchical wire-on-sheet α-Ni(OH) <sub>2</sub> nanoarrays as robust trifunctional catalysts for synergistic hydrogen generation and urea oxidation. Journal of Materials Chemistry A, 2019, 7, 13577-13584.	10.3	159
41	A ternary cobalt–molybdenum–vanadium layered double hydroxide nanosheet array as an efficient bifunctional electrocatalyst for overall water splitting. Chemical Communications, 2019, 55, 3521-3524.	4.1	121
42	Ni x Co 3―x O 4 Nanoneedle Arrays Grown on Ni Foam as an Efficient Bifunctional Electrocatalyst for Full Water Splitting. Chemistry - an Asian Journal, 2019, 14, 480-485.	3.3	21
43	Platinum Nanocrystals Decorated on Defect-Rich MoS <sub>2</sub> Nanosheets for pH-Universal Hydrogen Evolution Reaction. Crystal Growth and Design, 2019, 19, 60-65.	3.0	39
44	In situ detection of trace pollutants: a cost-effective SERS substrate of blackberry-like silver/graphene oxide nanoparticle cluster based on quick self-assembly technology. Optics Express, 2019, 27, 9879.	3.4	26
45	Removal of toxic metal ions using chitosan coated carbon nanotube composites for supercapacitors. Science China Chemistry, 2018, 61, 797-805.	8.2	23
46	Synthesis of low-cost 3D-porous ZnO/Ag SERS-active substrate with ultrasensitive and repeatable detectability. Sensors and Actuators B: Chemical, 2018, 256, 268-275.	7.8	55
47	Morphology and electronic structure modulation induced by fluorine doping in nickel-based heterostructures for robust bifunctional electrocatalysis. Nanoscale, 2018, 10, 20384-20392.	5.6	61
48	The CoMo-LDH ultrathin nanosheet as a highly active and bifunctional electrocatalyst for overall water splitting. Inorganic Chemistry Frontiers, 2018, 5, 2964-2970.	6.0	76
49	Two-Dimensional Mn-Co LDH/Graphene Composite towards High-Performance Water Splitting. Catalysts, 2018, 8, 350.	3.5	27
50	ZnCo2O4 ultrathin nanosheets towards the high performance of flexible supercapacitors and bifunctional electrocatalysis. Journal of Alloys and Compounds, 2018, 764, 565-573.	5.5	63
51	Capillarityâ€Assistant Assembly: A Fast Preparation of 3D Pomegranateâ€Like Ag Nanoparticle Clusters on CuO Nanowires and Its Applications in SERS. Advanced Materials Interfaces, 2018, 5, 1800672.	3.7	23
52	Partially amorphous nickel–iron layered double hydroxide nanosheet arrays for robust bifunctional electrocatalysis. Journal of Materials Chemistry A, 2018, 6, 16121-16129.	10.3	193
53	Ironâ€Incorporated αâ€Ni(OH) <sub>2</sub> Hierarchical Nanosheet Arrays for Electrocatalytic Urea Oxidation. Chemistry - A European Journal, 2018, 24, 18408-18412.	3.3	114
54	High stability luminophores: fluorescent CsPbX <sub>3</sub> (X = Cl, Br and I) nanofiber prepared by one-step electrospinning method. Optics Express, 2018, 26, 20649.	3.4	24

#	Article	IF	CITATIONS
55	Sub-3â€ <sup>-</sup> nm pores in two-dimensional nanomesh promoting the generation of electroactive phase for robust water oxidation. Nano Energy, 2018, 53, 74-82.	16.0	94
56	Visualization and Inhibition of Mitochondria-Nuclear Translocation of Apoptosis Inducing Factor by a Graphene Oxide-DNA Nanosensor. Analytical Chemistry, 2017, 89, 4642-4647.	6.5	13
57	Nano metal-enhanced power conversion efficiency in CH 3 NH 3 PbI 3 solar cells. Journal of Physics and Chemistry of Solids, 2017, 103, 16-21.	4.0	1
58	Dual Effect in Fluorineâ€Doped Hematite Nanocrystals for Efficient Water Oxidation. ChemSusChem, 2017, 10, 4465-4471.	6.8	51
59	Nitrogen-doping induced oxygen divacancies in freestanding molybdenum trioxide single-layers boosting electrocatalytic hydrogen evolution. Nano Energy, 2016, 30, 810-817.	16.0	62
60	Ultrathin TiO2 flakes optimizing solar light driven CO2 reduction. Nano Energy, 2016, 26, 692-698.	16.0	107
61	Metallic tin quantum sheets confined in graphene toward high-efficiency carbon dioxide electroreduction. Nature Communications, 2016, 7, 12697.	12.8	522
62	Innentitelbild: Metallic Single-Unit-Cell Orthorhombic Cobalt Diselenide Atomic Layers: Robust Water-Electrolysis Catalysts (Angew. Chem. 41/2015). Angewandte Chemie, 2015, 127, 12046-12046.	2.0	1
63	Metallic Singleâ€Unitâ€Cell Orthorhombic Cobalt Diselenide Atomic Layers: Robust Waterâ€Electrolysis Catalysts. Angewandte Chemie - International Edition, 2015, 54, 12004-12008.	13.8	166
64	Atomic‣ayerâ€Confined Doping for Atomicâ€Level Insights into Visibleâ€Light Water Splitting. Angewandte Chemie - International Edition, 2015, 54, 9266-9270.	13.8	158
65	Single Unit Cell Bismuth Tungstate Layers Realizing Robust Solar CO <sub>2</sub> Reduction to Methanol. Angewandte Chemie - International Edition, 2015, 54, 13971-13974.	13.8	342
66	Ultrathin Two-Dimensional Inorganic Materials: New Opportunities for Solid State Nanochemistry. Accounts of Chemical Research, 2015, 48, 3-12.	15.6	255
67	Atomically-thin two-dimensional sheets for understanding active sites in catalysis. Chemical Society Reviews, 2015, 44, 623-636.	38.1	872
68	Ultrahigh Energy Density Realized by a Singleâ€Layer βâ€Co(OH) <sub>2</sub> Allâ€Solidâ€State Asymmetric Supercapacitor. Angewandte Chemie, 2014, 126, 13003-13007.	2.0	32
69	Freestanding atomically-thin cuprous oxide sheets for improved visible-light photoelectrochemical water splitting. Nano Energy, 2014, 8, 205-213.	16.0	54
70	Allâ€5urfaceâ€Atomicâ€Metal Chalcogenide Sheets for Highâ€Efficiency Visibleâ€Light Photoelectrochemical Water Splitting. Advanced Energy Materials, 2014, 4, 1300611.	19.5	154
71	Ultrahigh Energy Density Realized by a Singleâ€Layer βâ€Co(OH) <sub>2</sub> Allâ€Solidâ€State Asymmetric Supercapacitor. Angewandte Chemie - International Edition, 2014, 53, 12789-12793.	13.8	290
72	Free-floating ultrathin tin monoxide sheets for solar-driven photoelectrochemical water splitting. Journal of Materials Chemistry A, 2014, 2, 10647.	10.3	54

#	Article	IF	CITATIONS
73	Photoelectrochemical Reactions: Allâ€Surfaceâ€Atomicâ€Metal Chalcogenide Sheets for Highâ€Efficiency Visibleâ€Light Photoelectrochemical Water Splitting (Adv. Energy Mater. 1/2014). Advanced Energy Materials, 2014, 4, .	19.5	3
74	Atomically-thin non-layered cobalt oxide porous sheets for highly efficient oxygen-evolving electrocatalysts. Chemical Science, 2014, 5, 3976.	7.4	332
75	Oxygen Vacancies Confined in Ultrathin Indium Oxide Porous Sheets for Promoted Visible-Light Water Splitting. Journal of the American Chemical Society, 2014, 136, 6826-6829.	13.7	1,178
76	Innentitelbild: Freestanding Tin Disulfide Single-Layers Realizing Efficient Visible-Light Water Splitting (Angew. Chem. 35/2012). Angewandte Chemie, 2012, 124, 8798-8798.	2.0	4
77	Freestanding Tin Disulfide Singleâ€Layers Realizing Efficient Visibleâ€Light Water Splitting. Angewandte Chemie - International Edition, 2012, 51, 8727-8731.	13.8	545